

Electronic Supplementary Information

Enhanced doping efficiency and thermoelectric performance of diketopyrrolopyrrole-based conjugated polymer with extended thiophene donors

Na Young Kim,^{a,1} Taek Seong Lee,^{b,1} Da Yeon Lee,^a Jong Gyu Oh,^b Keunjin Lee,^c Jae Young Kim,^d Tae Kyu An,^e Yong Jin Jeong,^{d,} Jaeyoung Jang^{b,*} Yun-Hi Kim^{a,*}*

^a Department of Chemistry and Research Institute for Green Energy Convergence Technology (RIGET), Gyeongsang National University, Jinju, 52828, Republic of Korea

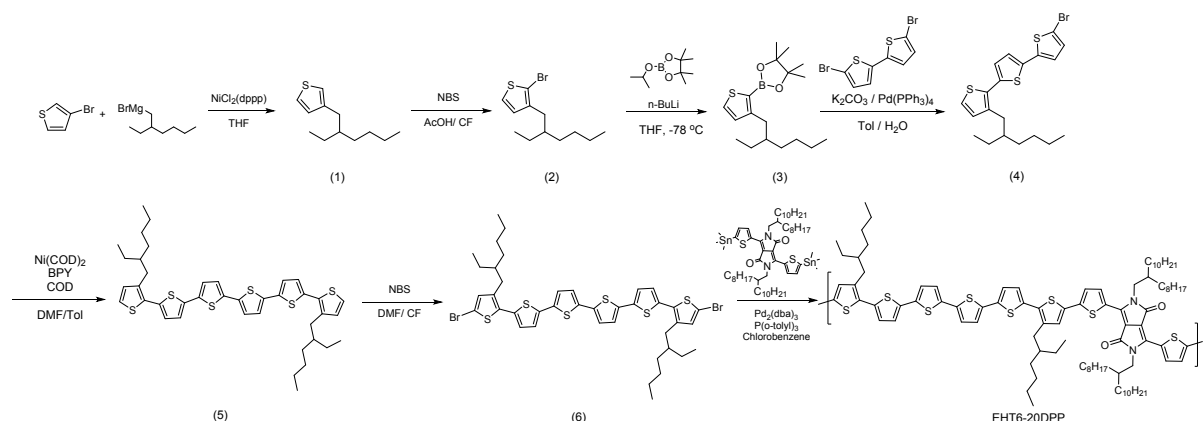
^b Department of Energy Engineering, Hanyang University, Seoul 04763, Republic of Korea.

^c Department of Materials Engineering and Convergence Technology and ERI, Gyeongsang National University, Jinju 660-701, Republic of Korea

^d Department of Materials Science & Engineering, Korea National University of Transportation, Chungju 27469, Republic of Korea.

^e Department of Polymer Science & Engineering, Korea National University of Transportation, Chungju 27469, Republic of Korea.

Synthesis of materials



Scheme S1. Synthetic route of EHT6-20DPP.

Materials

All reagents and solvents were purchased from Aldrich, Alfa aesar and TCI and used without further purification. And 2,5-bis(2-octyldodecyl)-3,6-bis(5-(trimethylstannyl)thiophen-2-yl)-2,5-dihydropyrrolo[3,4-c]pyrrole-1,4-dione (20DPP) was purchased from Derthon Optoelectronic Materials Science Technology Co LTD (Shenzhen, China).

Instruments

^1H NMR spectra were acquired using a Bruker 300 FT-NMR spectrometer and ^{13}C NMR spectra were recorded using a Bruker DRX 500 MHz spectrometer. HR mass analysis were obtained by a Joel JMS-700. Thermal gravimetric analysis (TGA) were performed using a TA 2050 TGA thermogravimetric analyzer under a nitrogen atmosphere with a heating rate of 10 $^\circ\text{C}/\text{min}$. Differential scanning calorimetry (DSC) was conducted under nitrogen atmosphere using a TA instrument 2100 DSC. The samples were heated at 10 $^\circ\text{C}/\text{min}$ from 10 $^\circ\text{C}$ to 300 $^\circ\text{C}$. UV-vis absorption spectra were measured using a Perkin-Elmer LAMBDA-900 UV/vis/IR spectrophotometer and photoluminescence spectra (PL) spectra were measured using a LS-50B luminescence spectrophotometer. Number average molecular weight (M_n) and weight average

molecular weight (Mw) were measured polystyrene standard using chloroform solvent by Waters GPC 2414.

Synthesis

(1) Synthesis of 3-(2-ethylhexyl)thiophene

Compound 1 was prepared according to the literature procedure.^{S1}

¹H-NMR (300 MHz, CD₂Cl₂) δ = 7.29-7.27 (m, 1H), 6.98-6.95 (m, 2H), 2.62 (d, J = 6.86 Hz, 2H), 1.64 (m, 1H), 1.36-1.29 (m, 8 H), 0.95-0.90 (m, 6H).

(2) Synthesis of 2-bromo-3-(2-ethylhexyl)thiophene

Compound 2 was prepared according to the literature procedure.^{S1}

¹H-NMR (300 MHz, CD₂Cl₂) δ = 7.26 (d, J = 5.61 Hz, 1H), 6.85 (d, J = 5.62 Hz, 1H), 2.56 (d, J = 7.19 Hz, 2H), 1.67-1.63 (m, 1H), 1.37-1.30 (m, 8H), 0.95-0.90 (m, 6H)

(3) Synthesis of 2-(3-(2-ethylhexyl)thiophen-2-yl)-4,4,5,5-tetramethyl-1,3,2-dioxaborolane

Compound 2 (2g, 7.27mmol) was dissolved in tetrahydrofuran (50 mL) in a round bottomed flask (100 mL) under the nitrogen atmosphere. n-BuLi (3.2 mL, 2.5 M in hexane) was added dropwise at -78 °C. The reaction mixture was maintained at -78 °C for 2 h. Then, 2-isopropoxy-4,4,5,5-tetramethyl-1,3,2-dioxaborolane (1.78 mL, 8.7 mmol) was added into the mixture and the mixture was stirred at -78 °C for 5 h. The mixture was poured into water and extracted with dichloromethane (3 × 100 mL). The organic solution was dried over anhydrous magnesium sulfate and concentrated under reduced pressure. The crude compound was purified by column chromatography on silica gel using dichloromethane/hexane (1:6, v/v) as eluent. Yield: 1.5 g

(64%)

$^1\text{H-NMR}$ (300 MHz, CD_2Cl_2) δ = 7.40 (d, J = 4.71 Hz, 1H), 6.92 (d, J = 4.72 Hz, 1H), 2.74 (d, J = 7.19 Hz, 2H), 1.50-1.43 (m, 1H), 1.23-1.14 (m, 20H), 0.80-0.75 (m, 6H). $^{13}\text{C NMR}$ (500 MHz, CD_2Cl_2): δ (ppm) = 153.79, 130.99, 130.85, 83.57, 41.50, 34.21, 32.55, 28.83, 25.60, 24.56, 23.13, 13.91, 10.45. HRMS (EI^+) m/z calcd for $\text{C}_{18}\text{H}_{31}\text{BO}_2\text{S}$, 322.2138; Found: 322.2137.

(4) Synthesis of 5''-bromo-3-(2-ethylhexyl)-2,2':5',2''-terthiophene

Under a nitrogen atmosphere, a solution of 2-(3-(2-ethylhexyl)thiophen-2-yl)-4,4,5,5-tetramethyl-1,3,2-dioxaborolane (1.5 g, 4.65 mmol), 5,5'-dibromo-2,2'-bithiophene (3.02 g, 9.31 mmol), and 2M K_2CO_3 in a dry toluene (50 mL) was deoxygenated with nitrogen for 20 min. $\text{Pd}(\text{PPh}_3)_4$ (0.27 g, 0.23 mmol) was added to the reaction and stirred at 100 °C for 18 h. After cooling room temperature, the mixture was extracted with dichloromethane (3×100 mL). The organic solution was dried over anhydrous magnesium sulfate and concentrated under reduced pressure. The crude product was purified by column chromatography on silica gel using n-hexane as eluent. Yield: 1 g (49%)

$^1\text{H-NMR}$ (300 MHz, CD_2Cl_2) δ = 7.13 (d, J = 5.21 Hz, 1H), 7.00 (d, J = 3.77 Hz, 1H), 6.94 (t, J = 8.0, 7.4 Hz, 2H), 6.86 (dd, J = 3.80, 4.48 Hz, 2H), 2.64 (d, J = 7.28 Hz, 2H), 1.61–1.50 (m, 1H), 1.24–1.15 (m, 8H), 0.80-0.73 (m, 6H). $^{13}\text{C NMR}$ (500 MHz, CD_2Cl_2): δ (ppm) = 139.52, 138.69, 135.89, 135.83, 130.85, 130.72, 130.56, 126.86, 124.22, 123.95, 123.73, 110.79, 40.34, 33.33, 32.55, 28.69, 25.78, 23.04, 13.85, 10.52. HRMS (EI^+) m/z calcd for $\text{C}_{20}\text{H}_{23}\text{BrS}_3$, 438.0145; Found: 438.0144.

(5) Synthesis of 3,3''''-bis(2-ethylhexyl)-2,2':5',2''':5'',2''':5''',2''''':5''''',2''''''-sexithiophene (EHT6)

Ni(COD)₂ (0.94 g, 3.41 mmol), 2,2'-bipyridine (0.53g, 3.41 mmol) and 1,5-cyclooctadiene (0.37 g, 3.41 mmol) were added into a flask and dissolved in 20 mL of anhydrous DMF. The solution was heated at 80 °C for 30 min. Then, toluene solution of compound 4 (1 g, 2.27 mmol) was added and stirred at 80 °C for 20 h. After cooling room temperature, the mixture was extracted with dichloromethane (3 × 100 mL). The organic solution was dried over anhydrous magnesium sulfate and concentrated under reduced pressure. The crude product was purified by column chromatography on silica gel using n-hexane. Yield: 1 g (61%)

¹H-NMR (300 MHz, CD₂Cl₂) δ = 7.27 (d, J = 5.21 Hz, 1H), 7.20 (d, J = 3.78 Hz, 1H), 7.17 (s, 2H), 7.09 (d, J = 3.78 Hz, 1H), 6.99 (d, J = 5.22 Hz, 1H), 2.79 (d, J = 7.28 Hz, 2H), 1.75–1.65 (m, 1H), 1.38-1.27 (m, 8H), 0.91-0.87 (m, 6H). ¹³C NMR (500 MHz, CD₂Cl₂): δ (ppm) = 139.42, 136.56, 136.07, 135.78, 135.59, 130.75, 130.55, 126.93, 124.44, 124.31, 123.98, 123.86, 40.35, 33.38, 32.58, 28.73, 25.80, 23.07, 13.88, 10.54. HRMS (FAB⁺) m/z calcd for C₄₀H₄₆S₆, 718.1924; Found: 718.1924

(6) Synthesis of 5,5''''-dibromo-3,3''''-bis(2-ethylhexyl)-2,2':5',2'':5'',2''':5''',2''''':5''''',2''''''-sexithiophene (EHT6-Br)

Compound 5 (0.5 g, 0.69 mmol) and N-bromosuccinimide (NBS; 0.25 g, 1.42 mmol) was dissolved in 100 mL of 1:1 mixture of acetic acid and chloroform and the mixture was stirred at room temperature overnight. Water was added to the reaction and the organic layer was washed with water and extracted with dichloromethane (3 × 100 mL). After the removal of solvent with rotary evaporator, the crude product was purified by column chromatography on silica gel using n-hexane. Yield: 0.5 g (82%)

¹H-NMR (300 MHz, CD₂Cl₂) δ = 7.19 (d, J = 3.80 Hz, 1H), 7.17 (s, 2H), 7.05 (d, J = 3.80 Hz, 1H), 6.95 (s, 1H), 2.71 (d, J = 7.38 Hz, 2H), 1.70-1.60 (m, 1H), 1.40-1.25 (m, 8H), 0.92-0.86 (m, 6H). ¹³C NMR (500 MHz, CD₂Cl₂): δ (ppm) = 139.96, 137.29, 136.05, 135.91, 134.01,

133.12, 132.21, 127.41, 124.48, 124.44, 123.90, 110.67, 40.34, 33.39, 32.55, 28.74, 25.73, 23.05, 14.14, 10.78. HRMS (FAB⁺) m/z calcd for C₄₀H₄₄Br₂S₆, 874.0134; Found: 874.0136

(7) Synthesis of EHT6-20DPP

Under a nitrogen atmosphere, a solution of 5,5''-dibromo-3,3''-bis(2-ethylhexyl)-2,2':5',2'':5'',2''':5''',2''''':5''''',2''''''-sexithiophene (0.15 g, 0.171 mmol) and 2,5-bis(2-octyldodecyl)-3,6-bis(5-(trimethylstannyl)thiophen-2-yl)-2,5-dihydropyrrolo[3,4-c]pyrrole-1,4-dione(0.2 g, 0.171 mmol) in a dry chlorobenzene (5 mL) was deoxygenated with nitrogen for 20 min. Pd₂(dba)₃ (3.13 mg, 0.0034 mmol) and P(o-tol)₃ (4.16 mg, 0.0137 mmol) were added to the mixture, and heated at 80 °C for 30 min. Afterwards, 2-(tributylstannyl)thiophene (0.1 mL) was added to the mixture for end-capping, and stirred for 3h. The reaction mixture was precipitated into methanol (300 mL with 0.2 M HCl aq). The crude polymer was filtered and purified by soxhlet extraction with methanol, hexane and toluene. The EHT6-20DPP was obtained by precipitation of the toluene solution into methanol. Yield: 0.15 g (55%) Mn = 22 kDa, Mw = 38 kDa, PDI =1.75) ¹H-NMR (500 MHz, CD₂Cl₂) δ = 7.54-6.66 (br, 14H), 4.21-3.85 (br, 4H), 2.18-2.12 (br, 12H), 1.31-1.06 (br, 100H)

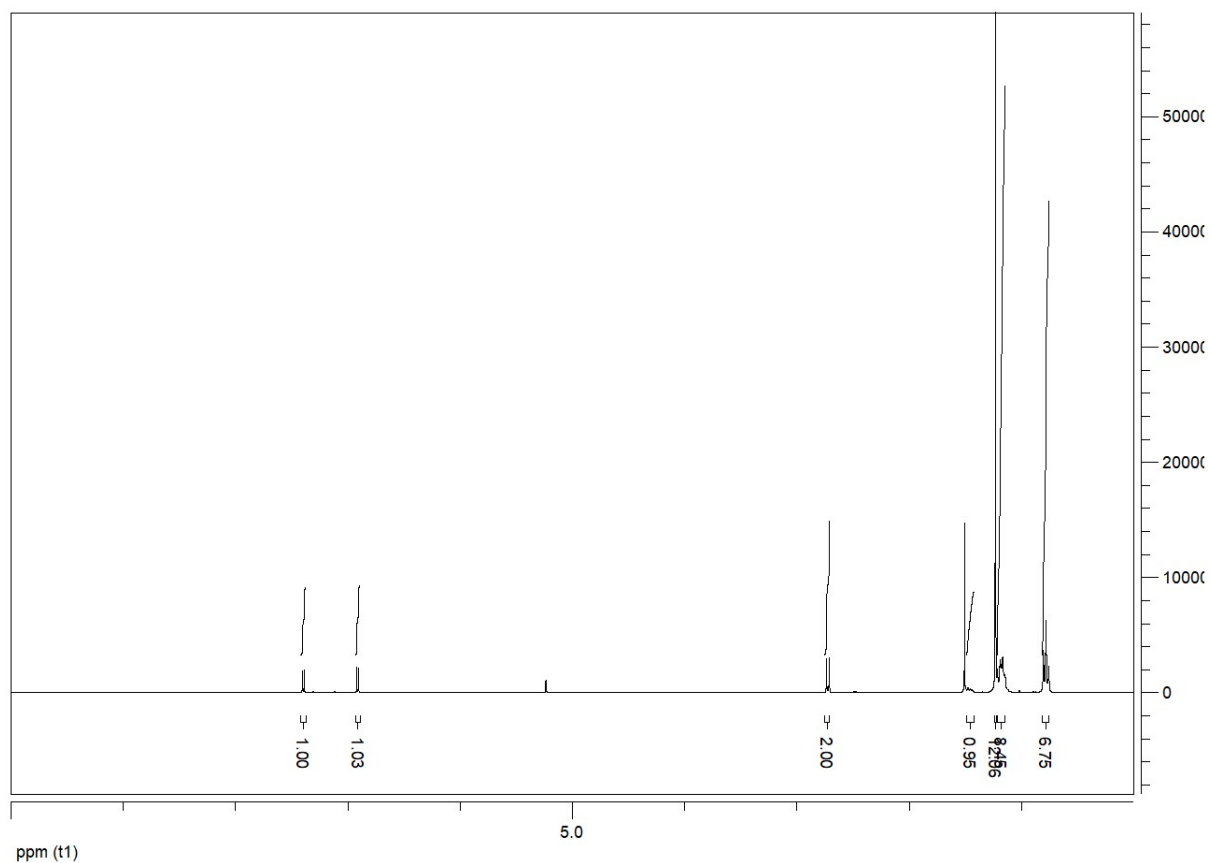


Figure S1. ¹H NMR data of 2-(3-(2-ethylhexyl)thiophen-2-yl)-4,4,5,5-tetramethyl-1,3,2-dioxaborolane.

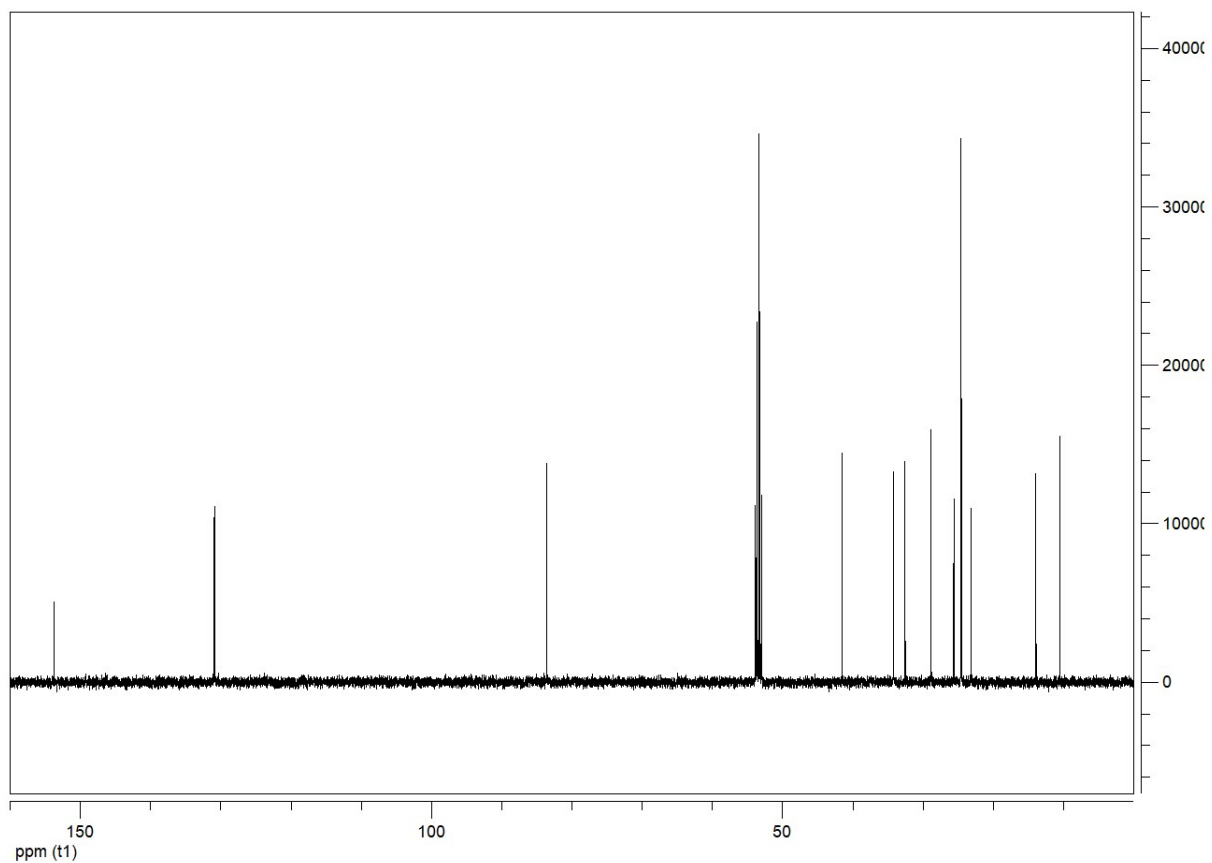


Figure S2. ^{13}C NMR data of 2-(3-(2-ethylhexyl)thiophen-2-yl)-4,4,5,5-tetramethyl-1,3,2-dioxaborolane.

[Mass Spectrum]
Data : eh-thio-Borate Date : 14-Apr-2020 13:48
Inlet : Direct Ion Mode : EI+
RT : 0.40 min Scan# : 13

Data : eh-thio-Borate_HR Date : 16-Apr-2020 16:11
Instrument : MStation
Sample : -
Note : -
Inlet : Direct Ion Mode : EI+
RT : 0.60 min Scan# : 10
Elements : C 100/1, H 100/1, O 4/1, S 4/1, 10B 1/0, 11B 1/0
Mass Tolerance : 1000ppm, 3mmu if m/z > 3
Unsaturation (U.S.) : -0.5 - 20.0

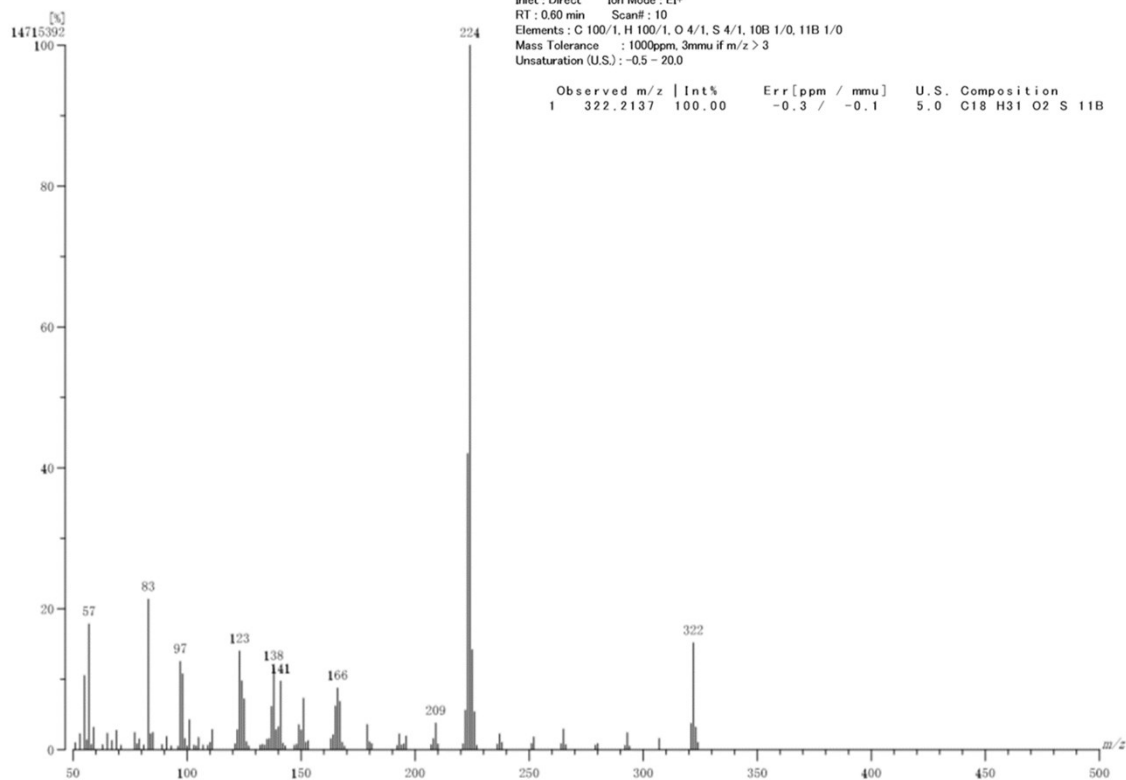


Figure S3. EI Mass spectrum of data of 2-(3-(2-ethylhexyl)thiophen-2-yl)-4,4,5,5-tetramethyl-1,3,2-dioxaborolane.

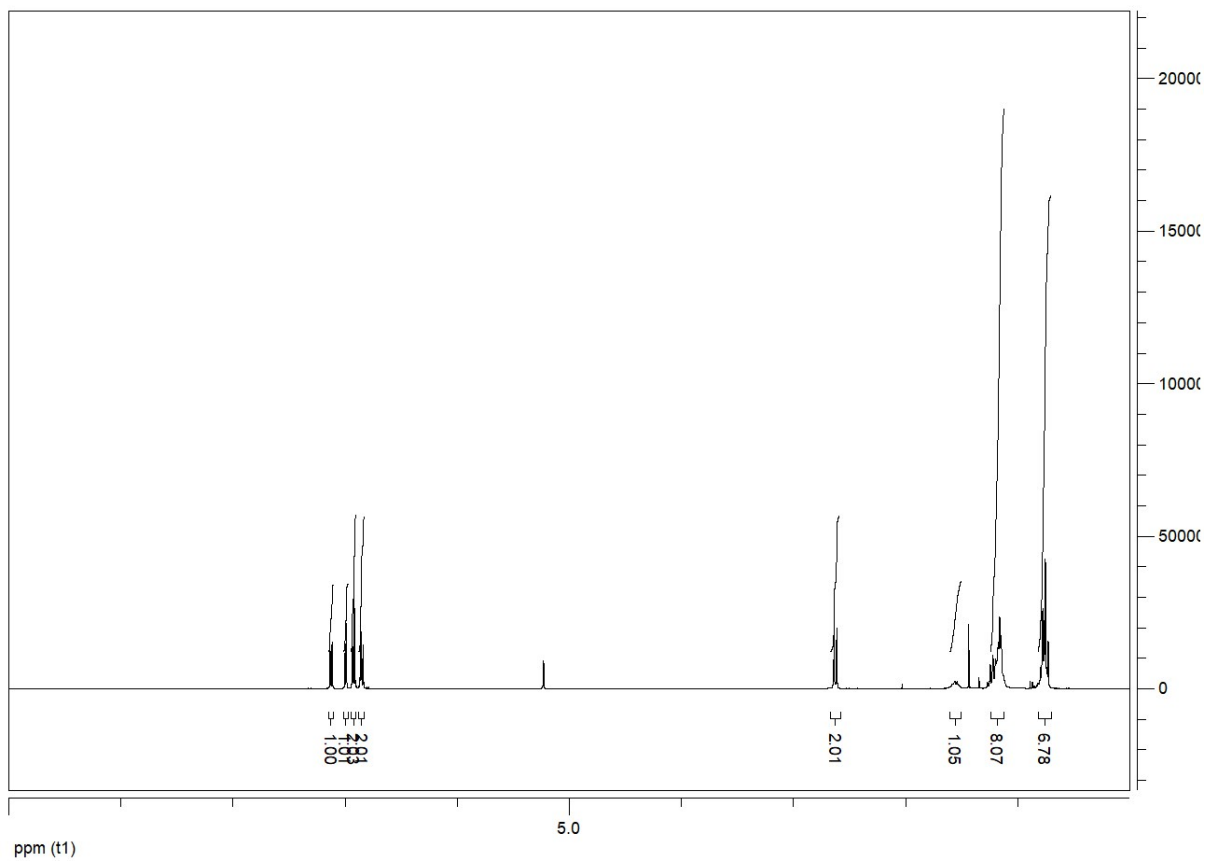


Figure S4. ^1H NMR data of 5-bromo-3-(2-ethylhexyl)-2,2':5,2''-terthiophene.

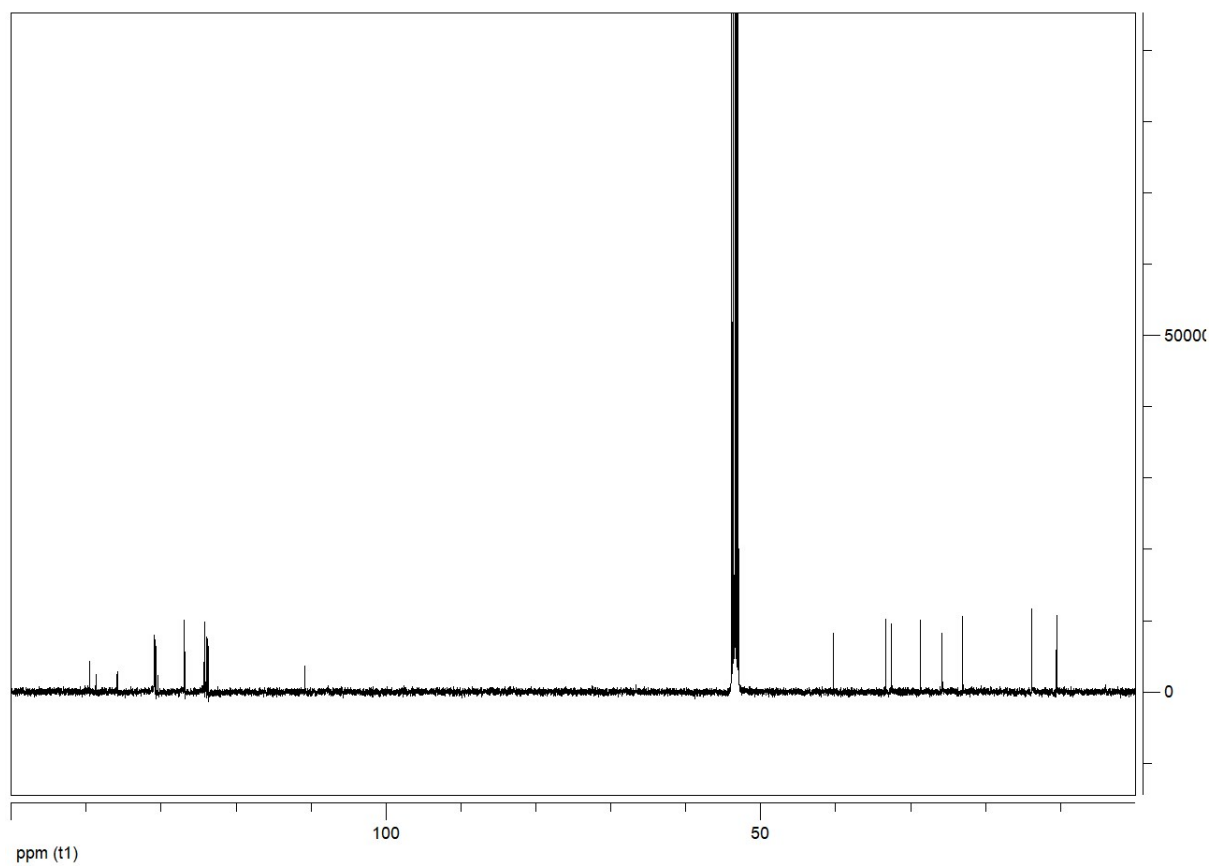


Figure S5. ^{13}C NMR data of 5''-bromo-3-(2-ethylhexyl)-2,2':5',2''-terthiophene.

[[Mass Spectrum]]
Data: eh-tert-thio-Br Date: 14-Apr-2020 13:56
Inlet: Direct Ion Mode: EI+
RT: 0.37 min Scan#: 12

Data: eh-tert-thio-Br.HR Date: 16-Apr-2020 16:22
Instrument: MStation
Sample: -
Note: -
Inlet: Direct Ion Mode: EI+
RT: 1.34 min Scan#: 21
Elements: C 100/1, H 100/1, 79Br 1/0, 81Br 1/0, S 3/1
Mass Tolerance: 1000ppm, 3mmu if m/z > 3
Unsaturation (U.S.): -0.5 - 20.0

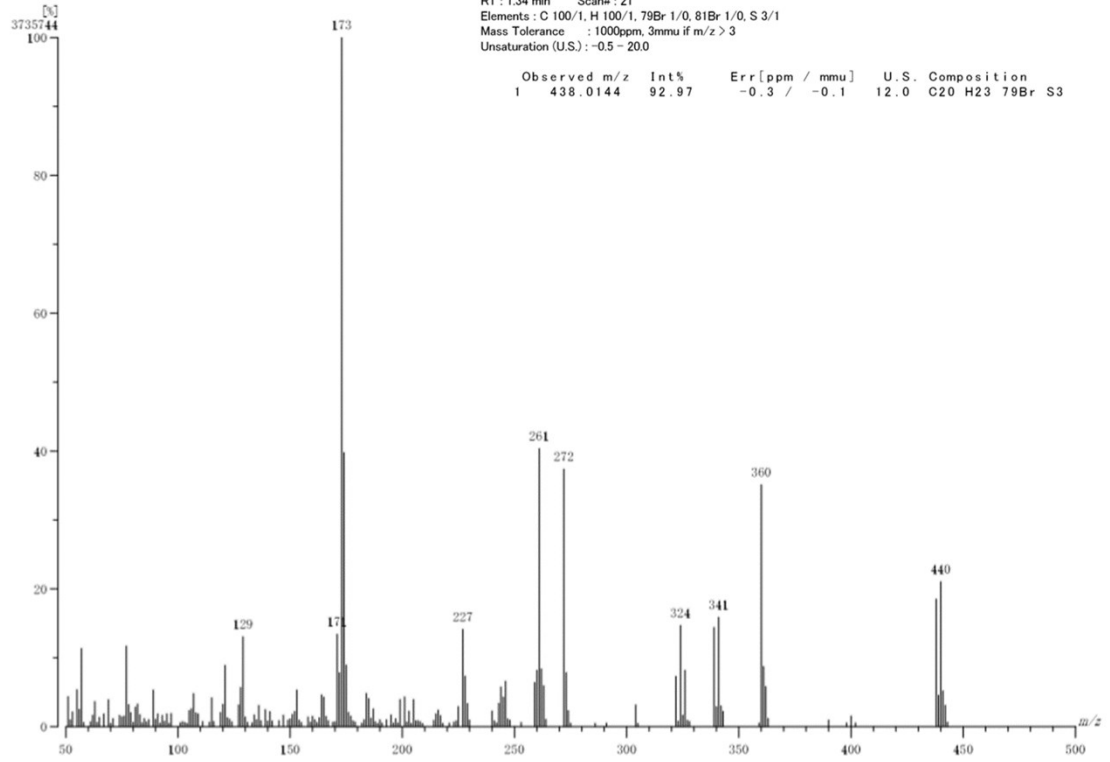


Figure S6. EI Mass spectrum of data of 5"-bromo-3-(2-ethylhexyl)-2,2':5',2"-terthiophene.

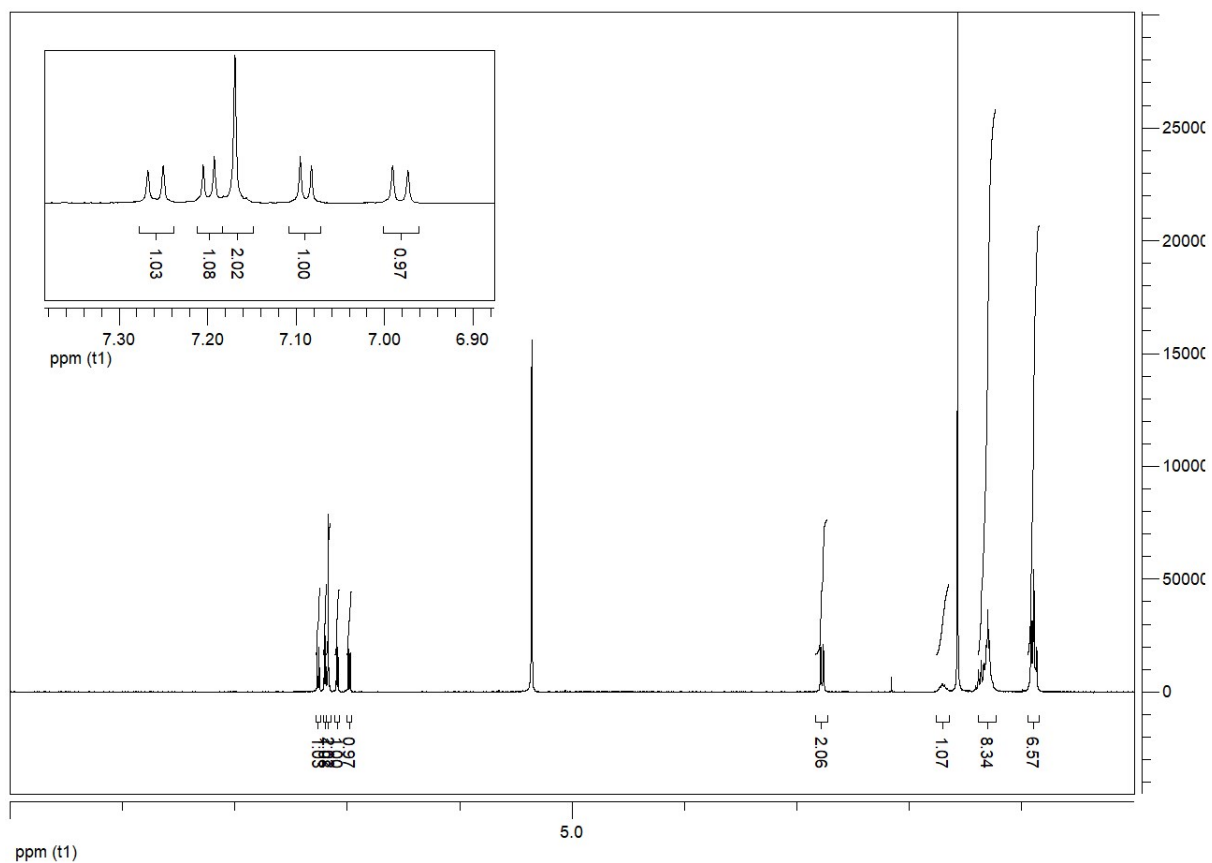


Figure S7. ¹H NMR data of 3,3'-bis(2-ethylhexyl)-2,2':5',2'':5'',2''':5''',2''''':5''''',2''''':5'''''-sexithiophene (EHT6).

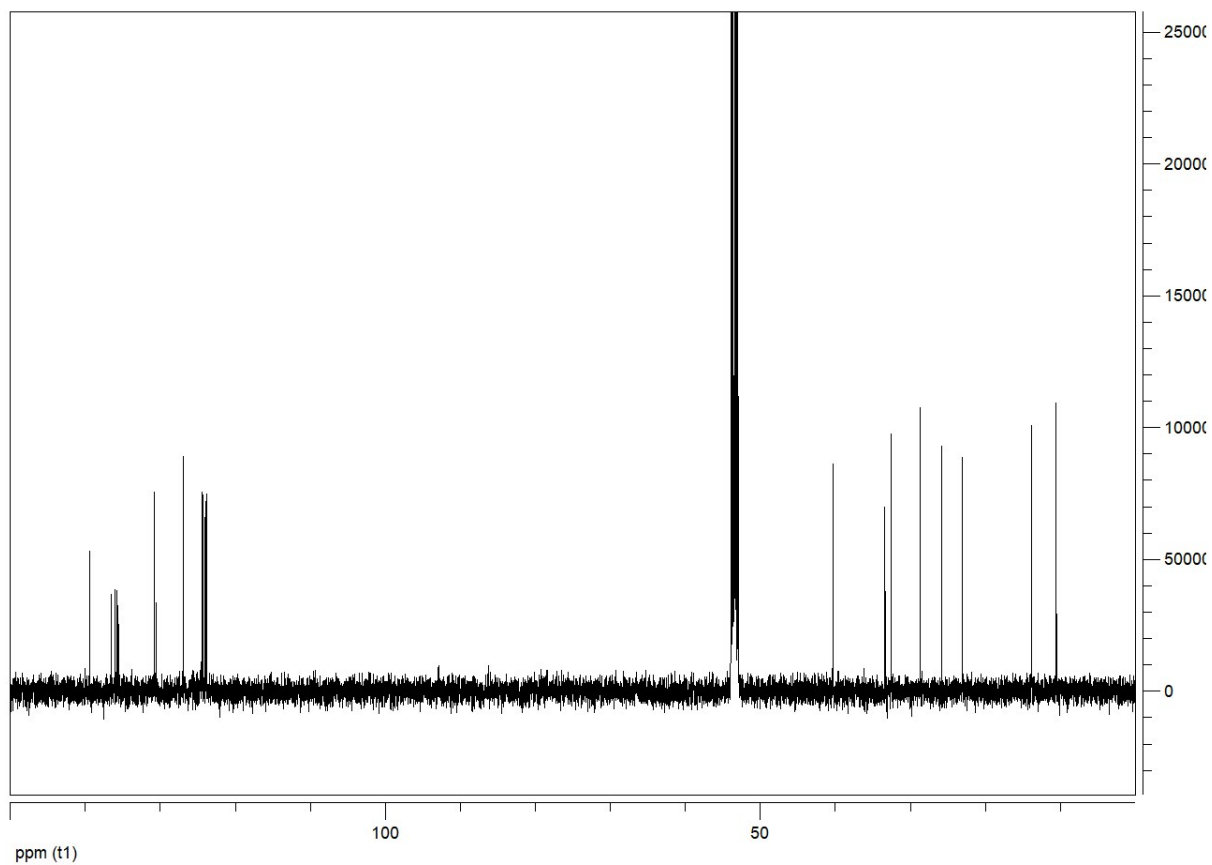


Figure S8. ^{13}C NMR data of 3,3''''-bis(2-ethylhexyl)-2,2':5',2'':5'',2''':5''',2''''':5''''',2''''''-sexithiophene (EHT6).

[Mass Spectrum]
Data : FAB-A110 Date : 20-Apr-2020 15:14
Instrument : MStation
Sample : EHT6
Note : m-NBA
Inlet : Direct Ion Mode : FAB+
Spectrum Type : Normal Ion [MF-Linear]
RT : 0.00 min Scan# : (1,3) Temp : 3276.7 deg.C
BP : m/z 154 Int. : 476.48 (4996224)
Output m/z range : 10 to 800 Cut Level : 0.00 %

[Mass Spectrum]
Data : FAB-A131 Date : 21-Apr-2020 15:01
RT : 0.03 min Scan# : (2,5)
Elements : C 100/0, H 100/0, S 8/4
Mass Tolerance : 1000ppm, 5mmu if m/z < 5, 10mmu if m/z > 10
Unsaturation (U.S.) : 10.0 - 30.0

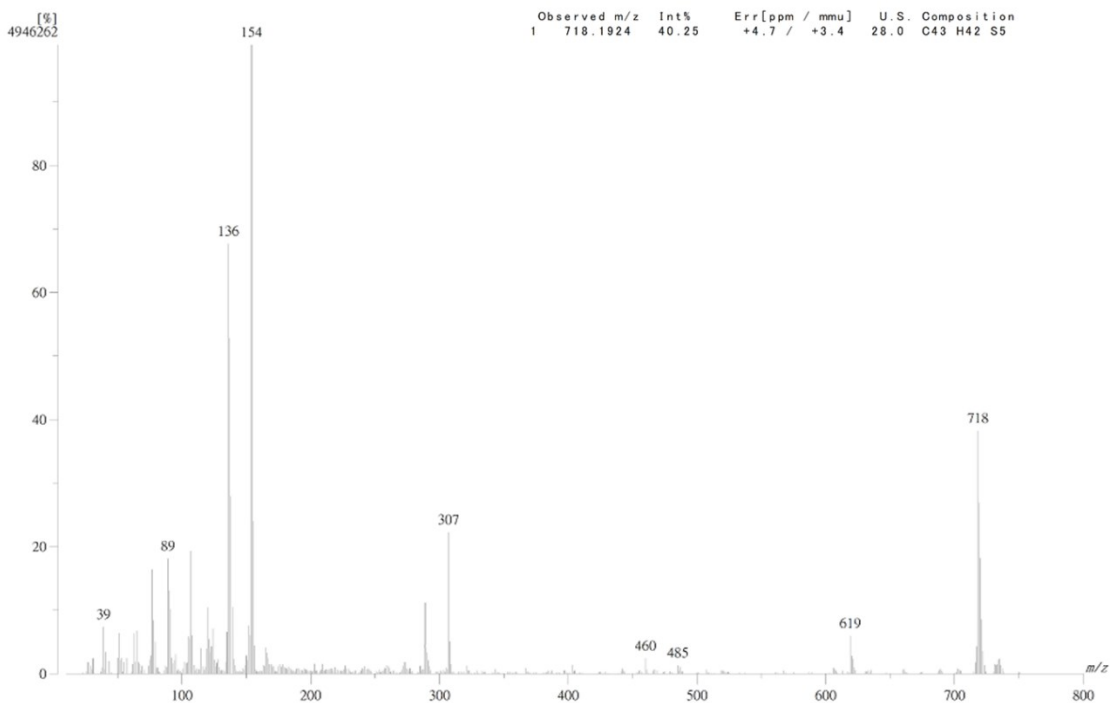


Figure S9. FAB Mass spectrum of data of 3,3''''-bis(2-ethylhexyl)-2,2':5',2'':5'',2''':5''',2''''-sexithiophene (EHT6).

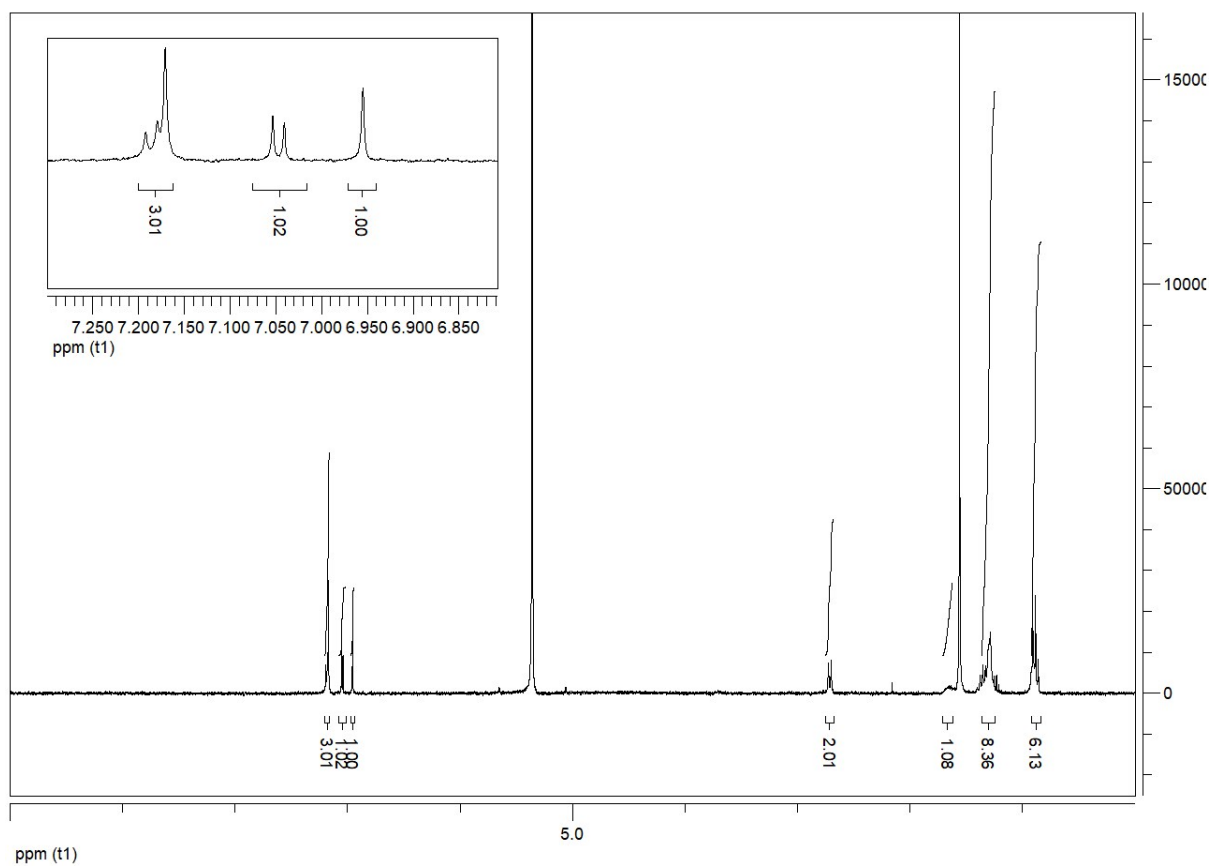


Figure S10. ^1H NMR data of 5,5'-dibromo-3,3'-bis(2-ethylhexyl)-2,2':5',2'':5'',2''':5''',2''''-sexithiophene (EHT6-Br).

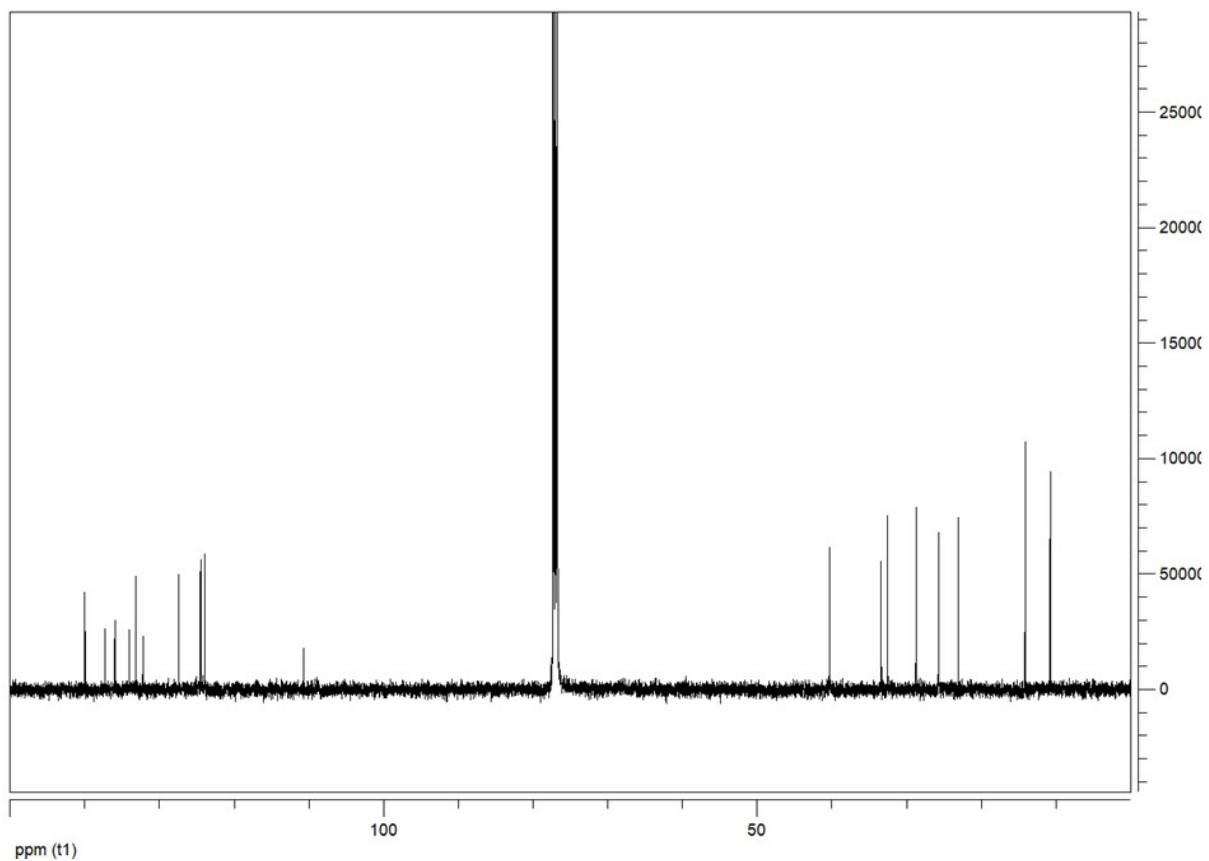


Figure S11. ^{13}C NMR data of 5,5''-dibromo-3,3''-bis(2-ethylhexyl)-2,2':5',2'':5'',2''':5''',2''''':5''''-sexithiophene (EHT6-Br).

[Mass Spectrum]
 Data : FAB-A095 Date : 17-Apr-2020 13:42
 Instrument : MStation
 Sample : EHT6-Br
 Note : m-NBA
 Inlet : Direct Ion Mode : FAB+
 Spectrum Type : Normal Ion [MF-Linear]
 RT : 0.60 min Scan# : (4,7) Temp : 3276.7 deg.C
 BP : m/z 154 Int. : 345.71 (3625072)
 Output m/z range : 10 to 951 Cut Level : 0.00 %

[Mass Spectrum]
 Data : FAB-A120 Date : 21-Apr-2020 10:51
 RT : 0.12 min Scan# : (5,23)
 Elements : C 100/0, H 100/0, 79Br 3/0, 81Br 3/0, S 8/0
 Mass Tolerance : 1000ppm, 5mmu if m/z < 5, 10mmu if m/z > 10
 Unsaturation (U.S.) : 15.0 - 35.0

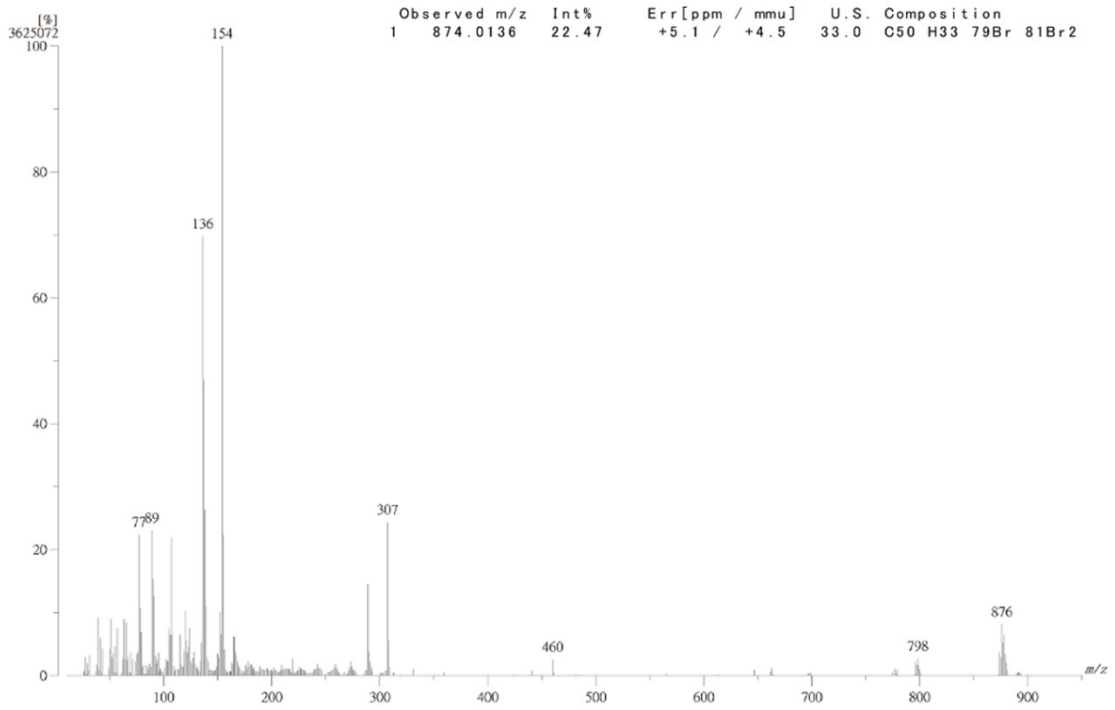


Figure S12. FAB Mass spectrum of data of 5,5''-dibromo-3,3''-bis(2-ethylhexyl)-2,2':5',2'':5'',2''':5''',2''''-sexithiophene (EHT6-Br).

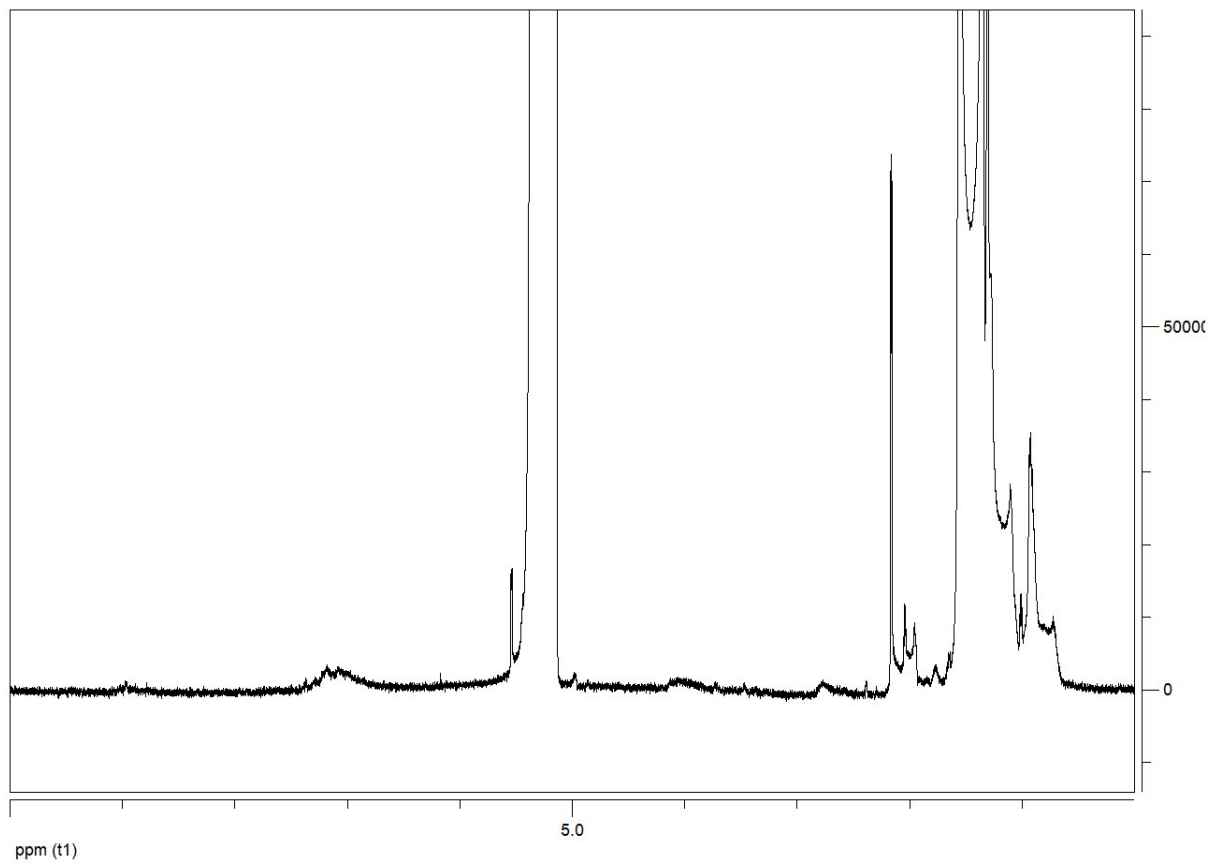


Figure S13. ^1H NMR data of EHT6-20DPP.



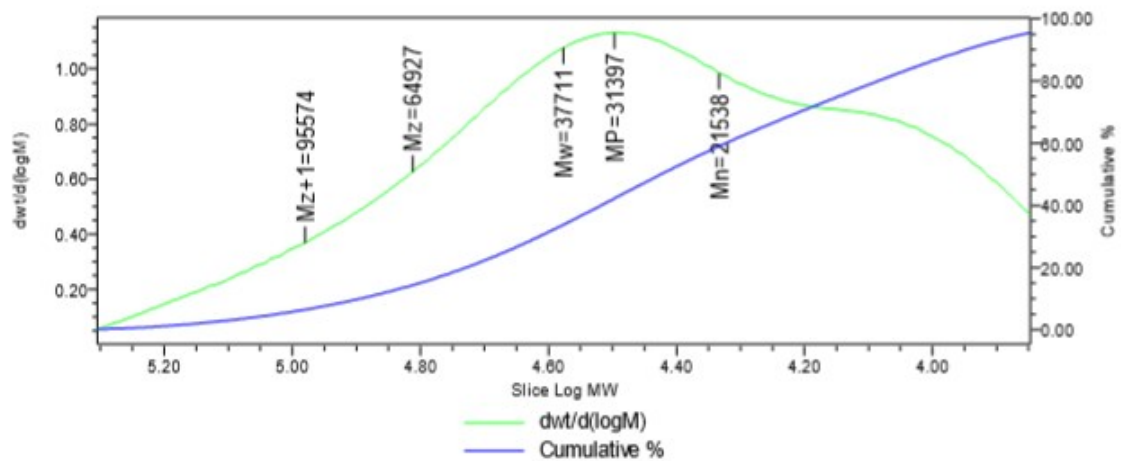
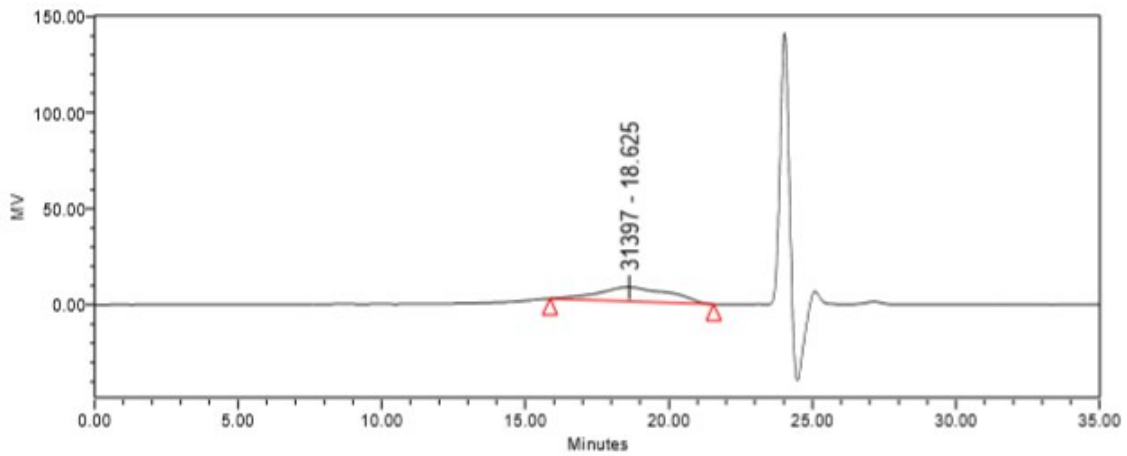
Individual GPC Sample Result

Reported by User: System

Project Name: NIM

SAMPLE INFORMATION

Sample Name:	eht6-dpp	Acquired By:	System
Sample Type:	Broad Unknown	Date Acquired:	2019-12-04 PM 11:29:16 KST
Vial:	5	Acq. Method Set:	NIM_Analysis
Injection #:	1	Date Processed:	2019-12-05 AM 12:14:13 KST
Injection Volume:	40.00 ul	Processing Method:	20191205
Run Time:	35.0 Minutes	Channel Name:	410
Sample Set Name:	20191204_ss	Proc. Chnl. Descr.:	410



GPC Results

Dist Name	Mn	Mw	MP	Mz	Mz+1	Mv	Polydispersity	MWMarker 1	MWMarker 2
1	21538	37711	31397	64927	95574		1.750882		

Figure S14. GPC data of EHT6-20DPP

Table S1. Physical properties of synthesized EHT6-20DPP.

Polymer	\bar{M}_w (KDa)	\bar{M}_n (KDa)	PDI	$E_{\text{HOMO}}^{\text{a)}$ (eV)	$E_g^{\text{b)}$ (eV)
EHT6-20DPP	38	22	1.75	-5.13	1.49

a) Cyclic Voltammogram of EHT6-20DPP-Tol films coated from chloroform solutions.

b) UV-vis spectra of as-cast EHT6-20DPP-Tol films spin coated from chloroform solutions.

Table S2. Summarized material characteristics of synthesized EHT6-20DPP.

UV-vis RT, a) (nm)	UV-vis 100°C, a) (nm)	UV-vis 150°C, a) (nm)	Molar extinction coefficient (cm^{-1} M^{-1})	T_d (°C)	T_g (°C)	T_m (°C)	T_c (°C)
760	760	756	63000	388	-	223	208

a) UV-vis absorption spectra of EHT6-DPP20-Tol films spin coated from chloroform solutions.

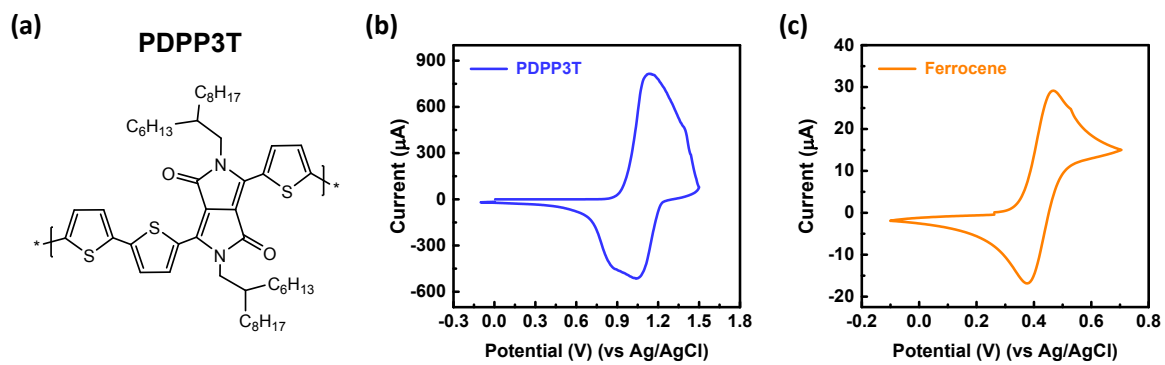


Figure S15. (a) Molecular structures of typical PDPP3T and (b) cyclic voltammograms of PDPP3T to analysis HOMO energy level.

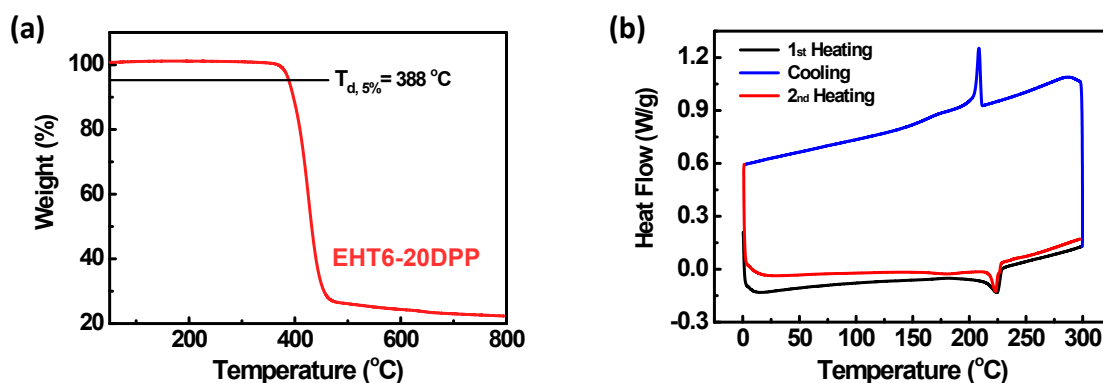


Figure S16. (a) Thermogravimetric analysis (TGA) plot of EHT6-20DPP and the black line shows 5 % weight decomposition temperature. (b) Differential scanning calorimetry (DSC) of neat EHT6-20DPP.

Table S3. Thickness of each sample depending on FeCl_3 doping concentration.

	FeCl_3 doping concentration (mM)								
	0	4	6	8	10	12	14	16	18
Thickness of EHT6-20DPP film (nm)	~93.9	~80.9	~83.7	~77.0	~70.5	~76.8	~82.2	~89.0	~93.4
Thickness of PDPP3T film (nm)	~81.5	~79.6	~108.0	~96.9	~88.3	~83.1	~88.1	~92.5	~113.0

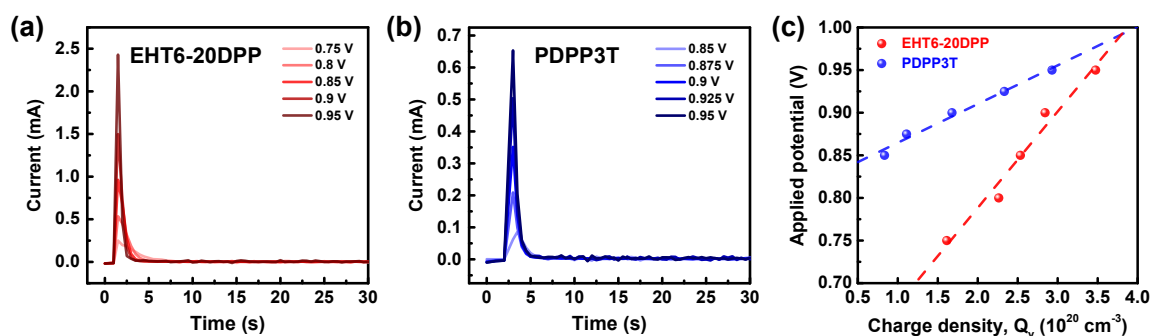


Figure S17. Time-dependent current behavior of (a) EHT6-20DPP and (b) PDPP3T under applying various potential, obtained from chronoamperometry. (c) Charge densities versus applied potential plots of both polymers.

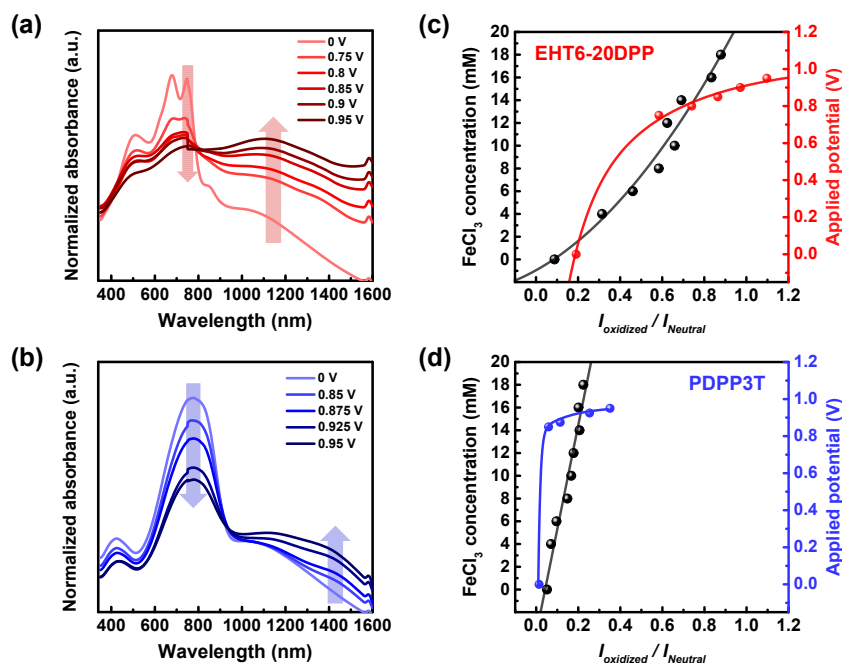


Figure S18. Thickness-normalized absorbance plots of (a) EHT6-20DPP and (b) PDPP3T films according to applied voltage. FeCl_3 concentration or applied potential *versus* the absorbance ratio between oxidized and neutral forms ($I_{\text{oxidized}}/I_{\text{neutral}}$) plots of (c) EHT6-20DPP and (d) PDPP3T films, showing the relation between FeCl_3 doping and electrochemical doping

The chronoamperometry may produce a meaningful information in terms of charge carrier density of polymer films. Chronoamperometry is a method of measuring generated current through applied static positive voltage which oxidizes the polymer, leading to the electrochemical doping.^{S2} To measure the current in chronoamperometry, three-electrode system would be used which is similar with the cyclic voltammetry measurement. It is consisting of indium tin oxide (ITO)/glass, Pt sheet, and Ag/AgCl electrodes, each of which operating as the working, counter, and reference electrodes, respectively. 0.1 M tetrabutylammonium hexafluorophosphate (Bu₄NPF₆) solution in acetonitrile was utilized as the electrolyte. Since the measured current was related to calculate the charge density through the electrochemical doping, the total number of charges Q would be calculated by integrating the measured current over time.

$$Q = \int_{t=0}^{\infty} I(t) dt \quad (1)$$

The charge density was obtained by dividing the total number of charges by volume of polymer films in contact with the electrolyte. From the cyclic voltammogram plots of EHT6-20DPP and PDPP3T in Figs. 1(b) and S15(b), they indicated the oxidation onset potential of ~0.75 V and ~0.85 V, respectively. The spin-coated polymer films on the working electrode immersed in the electrolyte for the chronoamperometry measurement, where we applied a series constant voltage for the oxidation reaction of both polymers. We performed the voltage from 0.75 V to 0.95 V in the case of EHT6-20DPP, whereas the voltage from 0.85 V to 0.95 V was added in PDPP3T. Before applying voltage for oxidation, we applied 0 V to polymer films for 100 s to set them to dedoped state. From Figs. S17(a) and S17(b) that exhibited the current behavior obtained from each polymer with applying potential, the calculated charge densities of both polymers depending on the applied potentials were plotted as shown in Fig. S17(c).

Since the charge density of EHT6-20DPP was higher at the same applied potential, it could indicate that the doping efficiency of EHT6-20DPP was better than PDPP3T directly.

After the electrochemical doping, the thickness-normalized absorbance plots of EHT6-20DPP and PDPP3T films according to applied voltage were drawn in Figs. S18(a) and S18(b), respectively. When the polymer films were oxidized with electrochemical doping, the absorbances of EHT6-20DPP and PDPP3T decreased at near 760 nm (neutral peak), but increased at 1140 nm and 1420 nm (oxidized peaks). As shown in Figs. S18(c) and S18(d), this electrochemical doping tendency of both polymer films seemed to be similar with the absorbance of FeCl₃ chemical doping (Figs. 2(a) and 2(b)), enabling electrochemical and chemical doping levels to be calibrated on the basis of the absorbance ratio between oxidized and neutral forms ($I_{oxidized} / I_{neutral}$). For example, doping EHT6-20DPP with 8 mM of FeCl₃ is corresponding to the electrochemical doping with applying ~0.75 V. Therefore, it could be estimated charge density of chemical doping system indirectly.

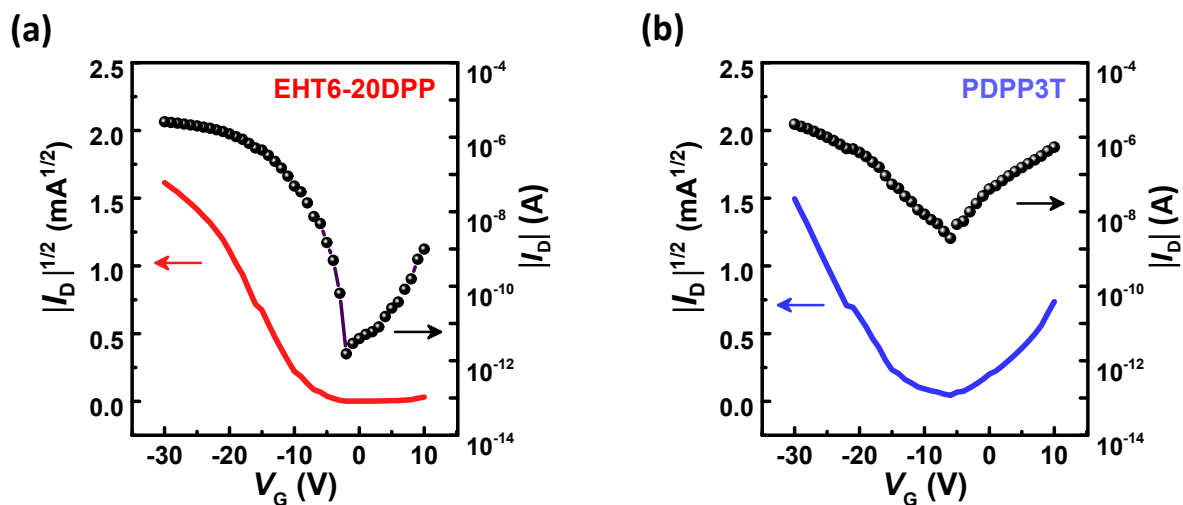


Figure S19. Transfer characteristics of the OFETs with the EHT6-20DPP and PDPP3T films.

Figure S19 shows transfer characteristics of the organic field-effect transistors (OFETs) with EHT6-20DPP and PDPP3T polymer films, respectively. The EHT6-20DPP and PDPP3T polymer thin films without FeCl₃ doping were used as active channels in the OFETs, after thermal annealing with 150 °C to remove solvents and to induce molecular self-assembly. Both OFETs displayed *p*-type transfer characteristics, whereas the OFETs with PDPP3T showed additional *n*-type transfer characteristics (i.e. ambipolar characteristics). The field-effect mobility in saturation region (μ_{FET}) was determined by fitting the experimental data of square-root drain currents ($I_{\text{D}}^{1/2}$) versus gate voltage (V_{G}) and using the following equation: $I_{\text{D}} = (WC_i/2L)\mu_{\text{FET}}(V_{\text{G}} - V_{\text{th}})^2$, where C_i is the capacitance per unit area of the octadecyltrichlorosilane-treated SiO₂ dielectric (30 nFcm⁻²) and V_{th} is the threshold voltage.

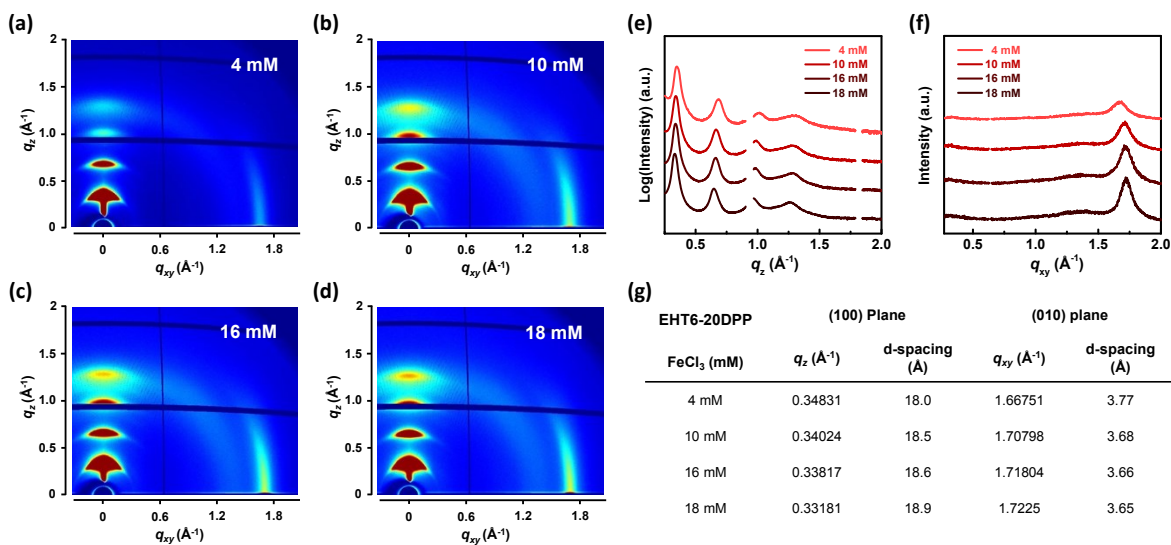


Figure S20. 2D-GIWAXS patterns of EHT6-20DPP films for doping concentration of (a) 4 mM, (b) 10 mM, (c) 16 mM, and (d) 18 mM and their cross-sectional intensity profiles of (e) out-of-plane and (f) in-plane direction. (g) Table of (100) and (010) peak values and d-spacing between each plane in EHT6-20DPP films with various dopant concentration.

In the doped states, d -spacing of (100) planes (d_{100}) of EHT6-20DPP films tended to increase from 18.0 Å (4 mM) to 18.9 Å (18 mM) with increasing FeCl₃ concentration. These results suggested the electrical conductivity might be decreased due to disturb the charge transport between polymer chain domains, inducing the scattering effect of charge carriers.^{S3,S4} Considering the above factors, we suggested from the UV-vis-NIR spectroscopy that the doping of EHT6-20DPP became saturated when the dopant concentration reached 16 mM; however, the electrical conductivity of EHT6-20DPP showed saturation over 10 mM dopant concentration because it was an optimized condition in dopant concentration between the generation of carriers and scattering effect.

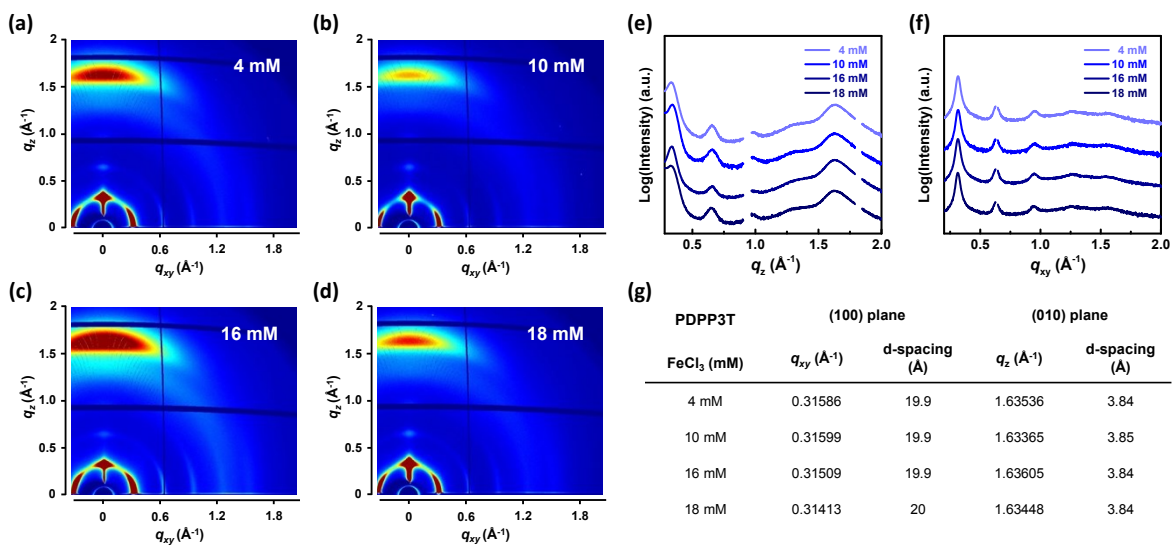


Figure S21. 2D-GIWAXS patterns of PDPP3T films for doping concentration of (a) 4 mM, (b) 10 mM, (c) 16 mM, and (d) 18 mM and their cross-sectional intensity profiles of (e) out-of-plane and (f) in-plane direction. (g) Table of (100) and (010) peak values and d-spacing between each plane in PDPP3T films with various dopant concentration.

Supplementary Reference

- S1.** T. Nakanishi, Y. Shirai, L. Han, *J. Mater. Chem. C*, 2015, **8**, 4229
- S2.** V. Untilova, J. Hynynen, A. I. Hofmann, D. Scheunemann, Y. Zhang, S. Barlow, M. Kemerink, S. R. Marder, L. Biniek, C. Muller and M. Brinkmann, *Macromolecules*, 2020, **53**, 6314-6321.
- S3.** J. Lee, J. Kim, T. L. Nguyen, M. Kim, J. Park, Y. Lee, S. Hwang, Y.-W. Kwon, J. Kwak and H. Y. Woo, *Macromolecules*, 2018, **51**, 3360–3368.
- S4.** X. Yan, M. Xiong, J. T. Li, S. Zhang, Z. Ahmad, Y. Lu, Z. Y. Wang, Z. F. Yao, J. Y. Wang, X. Gu and T. Lei, *J. Am. Chem. Soc.*, 2019, **141**, 20215–20221.